Pergamon PII: S0016-0032(97)00050-1

J. Franklin Inst. Vol. 335B, No. 6, pp. 1053–1068, 1998

Published by Elsevier Science Ltd
Printed in Great Britain
0016-0032/98 $19.00+0.00

An Integrated Method in Wavelet-based Image Compression

by HUNG-HSENG HSU,* YI-QIANG HU *and* BING-FEI WU

Department of Control Engineering, National Chiao Tung University, Hsinchu, Taiwan

(Received in final form 5 February 1997; revised 10 April 1997; accepted 1 May 1997)

ABSTRACT: *In this paper, we propose an integrated image compression method, which contains the discrete wavelet transform, scalar quantization and some lossless codings, to gain higher compression ratios while maintaining the image fidelity. The discrete wavelet transform has the properties of entropy reduction and energy concentration in high frequency subimages. An innovative approach, called revised run-length coding, is proposed to improve the compression performance. The idea of this approach is to represent the appearance of symbols of the run-length code in exponential expression for saving the storage in bits. The differential pulse code modulation is used to reduce the entropy of the lowest frequency subimage of the discrete wavelet transform and to achieve high compression effects losslessly.* © 1998 The Franklin Institute. Published by Elsevier Science Ltd

I. Introduction

A major objective of image compression is to represent an image by as few bits as possible while preserving the level of quality. Non-essential information is discarded to reduce the storage and transmission time in communication; see page 589 of (**1**). We usually compress an image as a prelude to either image storage or transport. This is because both of these operations are sensitive to the amount of data in an image; see page 179 of (**2**). Even though many compression techniques have been developed and implemented successfully up to now, there are still many innovative algorithms to be proposed based on the discrete wavelet transforms (DWT), which have been applied to the domain of image processing during the past ten years (**3**).

The fundamental idea behind the DWT is to analyze the signal according to scales and has the intention of a multiresolution technique; see page 399 of (**4**). From the application point of view, the DWT is regarded as one kind of the pyramid subband coding; see page 213 of (**5**). Also, the image can be split into different frequency

*To whom all correspondence should be addressed. E-mail: bwu@haeshiuh.cn.nctu.edu.tw, Tel.: +886-3-5712121, ext. 54313. Fax: +886-3-5712385.

components by the DWT. Each component, with a resolution matched to its scale, is considered as the DWT coefficient. The wavelet-based coding has been demonstrated to outperform other waveform based codings (**6**). We also derived the property of entropy reduction through the DWT (**7**). The effect of energy concentration in high frequency subimages is also observed; see page 373 of (**8**). Moreover, the histograms of the higher frequency subimages, which are called detailed images of the DWT, can be modelled to be generalized Gaussian distributed (**9**). The application of scalar quantization (SQ) extended the detailed images are motivated to obtain better compression conditions. This inherency of the DWT makes it interesting and useful to apply to image compression.

In this paper, we propose an integrated image compression method, which contains the DWT, SQ and some lossless codings, to gain higher compression ratios (CR) while maintaining the image fidelity. The (9,7) taps' wavelet, which belongs to the family of a spline variant with less dissimilar lengths, is chosen to be the basis of the DWT (**9**). In SQ, we introduce an optimal SQ (**10**) to increase the peak signal-to-noise ratio (PSNR), which is a performance index of the picture quality. Furthermore, some lossless codings, Huffman coding (HC), run-length coding (RLC) and differential pulse code modulation (DPCM) are provided to increase the CR without further distortion. We also combine the HC and RLC, denoted as HC+RLC, to achieve more compression effects than HC or RLC, separately. Meanwhile, an innovative approach, called revised run-length coding (RRLC), is proposed to lift the CR massively. The idea of RRLC is to represent the appearance of symbols of run-length codes in exponential expressions of base 2 for saving the storage in bits. It is also one kind of variable-length codings. The contribution of this paper is to provide an integrated compression technique, including the DWT, SQ, DPCM and lossless codings, to achieve higher compression performance and image fidelity. Comparisons of our approach with JPEG and other well-known approaches are also presented (**11–14**).

The organization of this paper is as follows. The flow chart of an integrated image compression procedure is portrayed in Section 2. The ideas of the integrated compression system are also discussed. In Section 3, we address the function of SQ and some coding methods individually. The innovative idea of RRLC, which expresses the run-length codes exponentially, is mentioned for more details. In Section 4, two testbed images, Lena and Mandrill, are considered to verify the increment of CR and PSNR performed after the integrated compression method. A concise conclusion is made in Section 5.

II. Image Compression by the DWT

In this paper, we consider the 3-layer DWT of an image, as shown in Fig. 1. A_3 represents to the lowest frequency subimage functioned after the DWT and D_{xi}, where x represents h, v or d, respectively, and $i = 1,2,3$, denotes the detailed images of each layer of the DWT. For A_3, the energy and the histogram are almost the same as those of the original image, since the energy of the image to be compressed is always concentrated in lower frequencies, in general. The coding method DPCM is suggested to maintain the image loyalty and to reduce the entropy of A_3. Hence, the HC is introduced to implement the entropy reduction. Moreover, since the histograms of

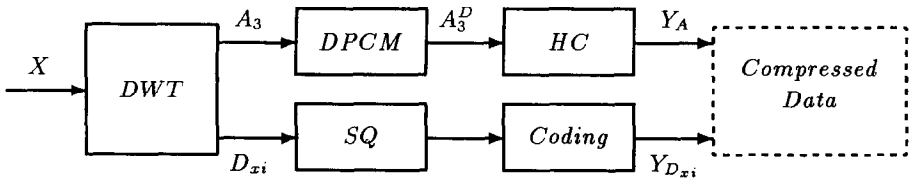

FIG. 1. The 3-layer DWT.

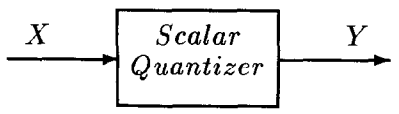

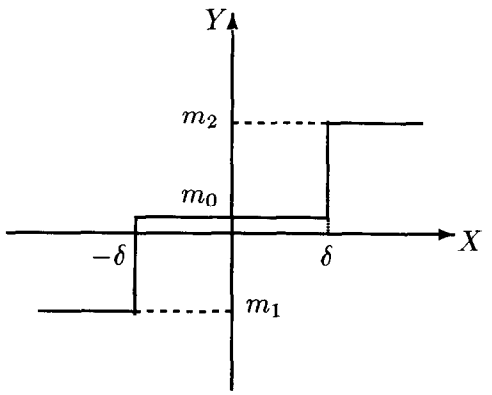

FIG. 2. The integrated image compression system.

detailed images satisfy the generalized Gaussian distributions (**9**), we introduce the SQ to compress the data with little distortion. There needs for some lossless coding methods to obtain further compression effects. Our intention is to derive the integrated compression system, as shown in Fig. 2. The component *Coding* in Fig. 2 represents one of the methods, HC, RLC, RLC+HC or RRLC.

After the image is transformed by the DWT, the subimages A_3 and D_{xi} are obtained directly. The information contained in A_3 is important so that the lossless coding methods behind A_3 are suggested to prevent any further distortion. Moreover, the histogram of A_3 and that of the original image are almost the same. It reveals that both entropies are approximately equal (**7**). When the DPCM is adopted, the entropy of A_3 can be reduced apparently. In addition, A_3^D, the output of DPCM, has a largely reduced variance compared with A_3; see page 61 of (**15**). Following that, the function of HC, which is a lossless coding method, is adopted to obtain the data Y_A.

The histograms of D_{xi} can be modelled as the generalized Gaussian distributions (**9**). Consequently, the 3-level scalar quantizer in Fig. 3, which shows three output levels of

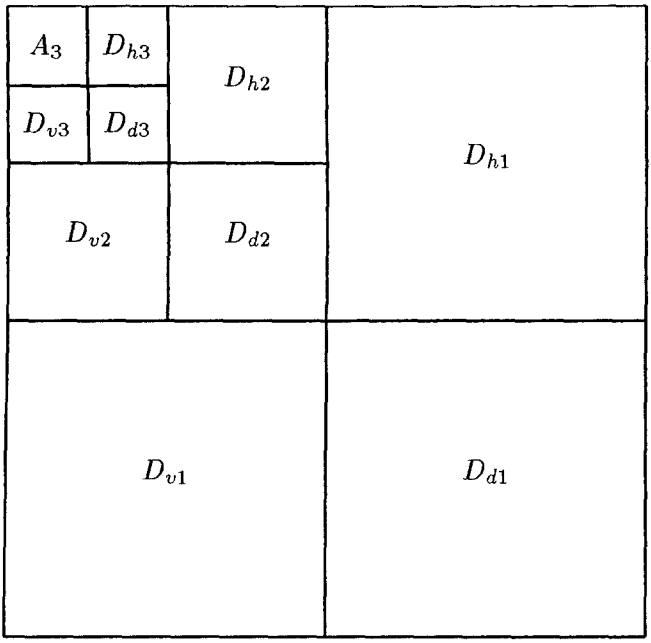

FIG. 3. The I/O characteristic of the 3-level scalar.

the quantizer, is introduced to gain better compression performance at the cost of producing some quantization error. The global minimum of quantization error can be obtained by using algorithms presented in our previous work (**10**). Furthermore, lossless coding methods are provided to reach higher compression ratios without any loss of quality. The output generated by these lossless coding is denoted by D_{xi}.

III. Quantization and Lossless Codings

The fundamental ideas of scalar quantization and lossless codings will be addressed in the following discussions.

3.1. *Optimal SQ*

The previous section mentions that every detailed image D_{xi} could be quantized by the 3-level scalar quantizer with symmetrical decision levels, since these histograms of the detailed images can be modelled as the generalized Gaussian distributions. SQ is the only component to introduce error during the whole process of image compression. The performance index PSNR is usually used in image coding and defined as follows:

$$\text{PSNR} = 10 \log_{10} \frac{255^2}{\text{MSE}},$$

where MSE is the abbreviation of mean squared error. The optimal value of PSNR can be obtained for choosing suitable decision level and reconstructed levels of SQ

(**10**). The higher the values of PSNR, the better the fidelities of the reconstructed images. Unfortunately, higher values of PSNR usually lead to worse values of CR. Hence, we need to deviate the value of decision level from the optimal value to obtain better CR.

3.2. *Lossless codings*

3.2.1. *DPCM coding.* In general, the information contained in the lowest frequency component of the 3-layer DWT, A_3, is rich enough such that we cannot conduct any further distortion by the lossy compression technique. The histogram and entropy of A_3 are almost the same as those of the original picture. The lossless coding DPCM could be introduced, since the histogram of the output of DPCM is highly concentrated around zero and resembles the Laplacian distribution (see page 78 of (**16**)) of the form

$$P(x) = \frac{1}{\sqrt{2}\sigma} \exp(-\sqrt{2}|x|/\sigma),$$

where σ^2 is the variance of the distribution. In general, the histograms of the output of DPCM corresponding to different images have roughly the same shapes but different variances (**15**). Obviously, the entropy and standard deviation are heavily reduced after DPCM, as shown in Fig. 4. The entropy and standard deviation of Lena are 7.3039 bpp (bits per pixel) and 44.0826, respectively. After DPCM, the entropy and standard deviation are 4.9476 bpp and 10.9551, respectively. It implies that we have the opportunity to gain the lossless compression ratios of $8/4.9476 = 1.6169$ instead of $8/7.3039 = 1.0953$. Hence, the DPCM is adopted by the lowest frequency component to reach the better compression conditions without generating any more distortion. Apparently, the HC will be adopted to perform the entropy reduction after DPCM.

3.2.2. *RRLC.* There are three kinds of output levels, m_0, m_1 and m_2, when a detailed image is quantized by a 3-level scalar quantizer. For convenience, m_0, m_1 and m_2 are represented by 0, -1 and 1, respectively. A value of the input signal which is less than $-\delta$ is mapped to the symbol -1, a value which lies in the interval of $[-\delta,\delta]$ is denoted by the symbol 0 and a value which is larger than δ is represented by the symbol 1. Actually, the probability of appearance of the symbol 0 is higher than that of each of

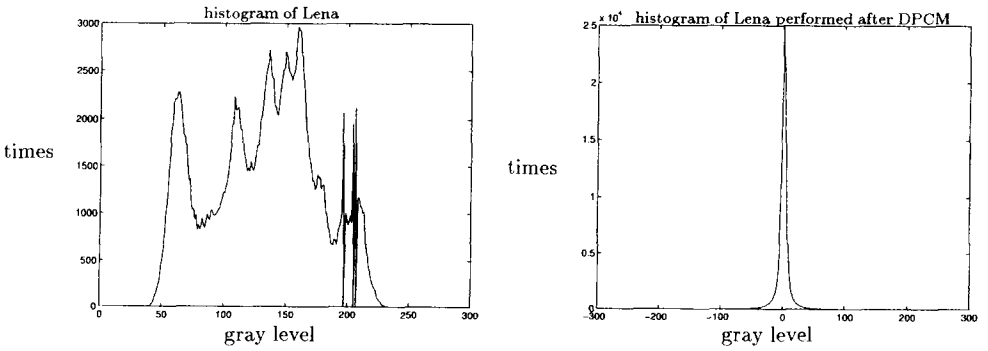

FIG. 4. The histograms of Lena and Lena + DPCM.

the other symbols since the histograms of the detailed images concentrate at the neighborhood around zero.

The detailed images, which contain the higher frequency components, pick the edge in the spatial domain of the original image. An edge in the image is a boundary or contour at which a significant change occurs in some physical aspect of the image. Hence, the detailed images performed after the DWT have the intent of edge detection in image processing. That is, the values which are mapped to the symbol 1 or -1 characterize that the change of the image intensities are positive or negative, respectively, in the spatial domain of the original image. Moreover, the values which are symbolized by 0 describe the smoothing parts of the original picture. For example, the image of Lena seems to have many connected areas which deal with low spatial frequencies. Hence, a lot of symbols 0 will be generated continuously in these detailed images. The coding method RLC is helpful to process this situation.

In RLC process, both the symbol and the number of appearances of the symbol should be stored as a code. For example, in the case of D_{d_1} in Lena, the gray levels after the 3-level scalar quantizer with decision level equal to 10.6 are as follows:

$$\overbrace{0,\ldots,0}^{30105},1,1,1,-1,-1,-1,-1,\ldots.$$

The run-length codes are shown in the sequence

$$(0;30105),(1;3),(-1;4),\ldots.$$

In each pair of parentheses, the former is for the symbol and the latter is for the number of appearances. Since the symbols and the appearance frequencies can be distinguished from the location point of view, we encode the symbols 0, 1 and -1 as 00, 01 and 11, respectively. However, the appearance frequencies of symbols are unpredictable in real cases. It is troublesome in bit allocations. By the above example, the number of appearances should be assigned by 15 bits, which are the minimum bits to encode the value of 30105. That is, the binary representation of 30105 is 111,010,110,011,001. It is not economical to encode the values of 3 or 4 by 15 bits since they could be encoded by 2 bits only, in practice. The total bits we need to represent the three run-length codes are $(2+15)\times 3 = 51$. This is the so-called fixed-length coding. The RRLC method is proposed to solve this problem by representing the appearance frequencies exponentially and is a kind of variable-length codings.

The idea of RRLC is to depict the appearance rate by exponential codes with base 2 for saving the bits we need. A group of revised run-length codes include data codes (d-code, 2 bits/code), appearance codes (a-code, a bits/code), page codes (p-code, p bits/code) and an identification code (id-code, 10). Hence, the revised run-length codes are of the form

$$\underbrace{\square\square}_{d\text{-}code},\underbrace{\overbrace{\triangle\ldots\triangle}^{a}}_{a\text{-}code},\underbrace{\square\square}_{d\text{-}code},\underbrace{\overbrace{\triangle\ldots\triangle}^{a}}_{a\text{-}code},$$

for the value of appearance rate less than or equal to 2^{2a}, or

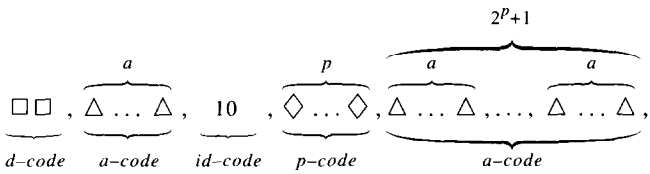

for the value of appearance rate greater than 2^{2a}, where □, △ and ◇ represent the data bit, appearance bit and page bit, respectively. For example, we consider the case with $a = 3$ and $p = 2$. Hence, the pair of (0;30105) can be encoded as

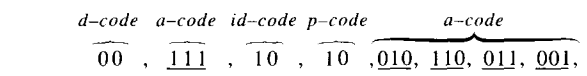

where these 15 bits, which are marked by the underlinings, represent the binary expansion of 30105. Using this strategy, the run-length code of (0;30105) can be encoded by 21 bits. Moreover, the run-length codes of (1;3) and (−1;4) are encoded as 01, 011 and 11, 100, respectively. The total bits we need to encode the three pairs of run-length codes are $21 + 5 + 5 = 31$ bits which is less than the 51 bits generated by the fixed-length coding. If the changes of the number of appearances are large enough such that we cannot code them by fixed numbers of bit allocation efficiently, the RRLC method is better than the traditional RLC method.

IV. Experimental Results

Two examples of 2-D images, Lena and Mandrill, are provided to illustrate the results which have been discussed before. The testbed images are of 512×512 pixels with 8-bit gray levels. The filters for the DWT are (9,7) taps' filters which belong to the family of a spline variant (**9**). The structure of the DWT follows Mallat's algorithm (**3**), which deals with the 2-D image problems and which is a kind of pyramid subband codings. Here, A_1 represents the lowest frequency subimage of the first layer (resolution 1/2) DWT decomposition, and D_{h_1}, D_{v_1} and D_{d_1} are the horizontal, vertical and diagonal oriented subimages with resolution 1/2, respectively.

4.1. *The choice of* δ

The increment of PSNR brings about the decrement of CR, in general. That is a trade-off problem. Suppose that we choose the optimal value of decision levels δ^*, which is the value of δ such that the MSE is minimum; then CR is usually very low. To overcome the drawback of lower values of CR, the values of δ should be altered for increasing CR. In our previous work (**17**), the entropy of the output signal performed after a 3-level scalar quantizer has a global maximum $\log_2 3$ if the input signals of the quantizer, i.e. detailed images, are generalized Gaussian distributed. The entropy can be considered as the lowest bound of bpp which has the similar meaning to CR. Hence, we can reduce the entropies or raise CR by enlarging the values of δ. See Fig. 5 for more details. For the case of Lena in Table 1, the value of δ increases from 5.403 to 10.6 to obtain a better CR under the condition that PSNR is still over 30 dB. In order

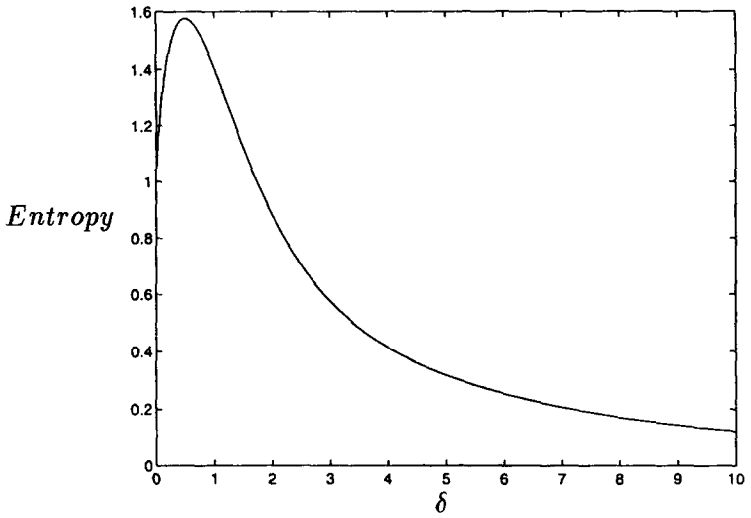

FIG. 5. Entropy vs δ in Lena.

TABLE I
CR and PSNR with different values of δ

Testbed pictures	Lena		Mandrill	
	$\delta_{opt} = 5.403$	$\delta = 10.6$	$\delta_{opt} = 6.256$	$\delta = 19.7$
CR	20.2721	37.8958	5.6567	17.6439
PSNR	31.1371	30.0203	25.4446	22.5076

to maintain the PSNR over 22.5 dB for the case of Mandrill, the value of δ can be chosen as 19.7. The relationships of PSNR and CR in Lena and Mandrill with δ increase from 3 to 12 and 24, respectively, are shown in Fig. 6. The original pictures and reconstructed pictures with different PSNRs of Lena and Mandrill are shown in Figs 7 and 8, respectively.

4.2. *Improvement of* A_3 by DPCM

In order to reduce the entropy of A_3 for further compression, the concept of DPCM, which is a lossless compression, is introduced. Figure 9 shows that the energy of A_3 has been concentrated after DPCM. Moreover, the entropy and standard deviation reduction of these two testbed pictures are shown in Table 2. By the good characteristic of DPCM, the HC is used to increase the CR of A_3. Actually, the CR of the overall compression system is raised from 33.7439 to 37.8958 in the case of Lena.

4.3. *Compression by HC, RLC, RLC+HC and RRLC*

HC and RLC are the popular lossless codings in image compression, and can behave well for the condition of lower entropies and for contiguous symbols in spatial domain,

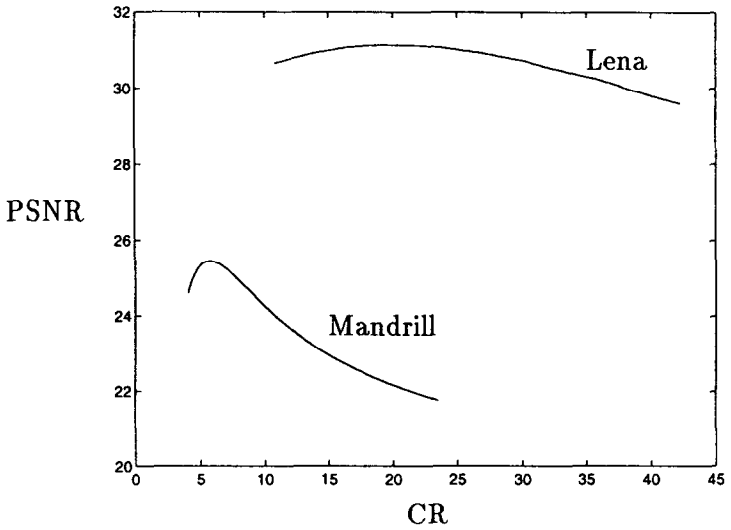

FIG. 6. Curves of PSNR vs CR in Lena and Mandrill.

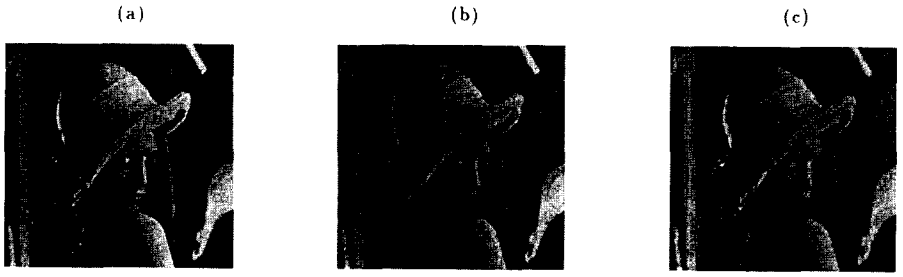

FIG. 7. (a) Original Lena and the reconstructed pictures with (b) PSNR = 31.1371, (c) PSNR = 30.0203.

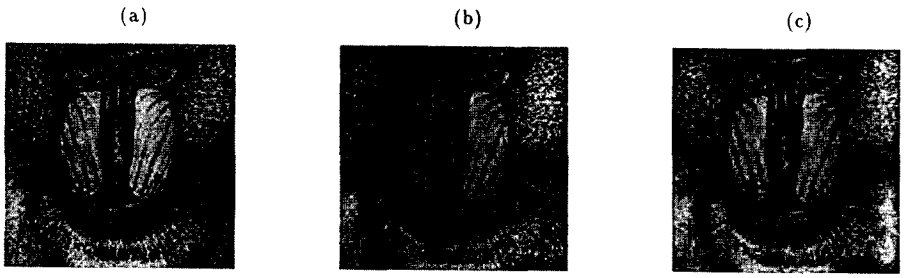

FIG. 8. (a) Original Mandrill and the reconstructed pictures with (b) PSNR = 25.4446, (c) PSNR = 22.5076.

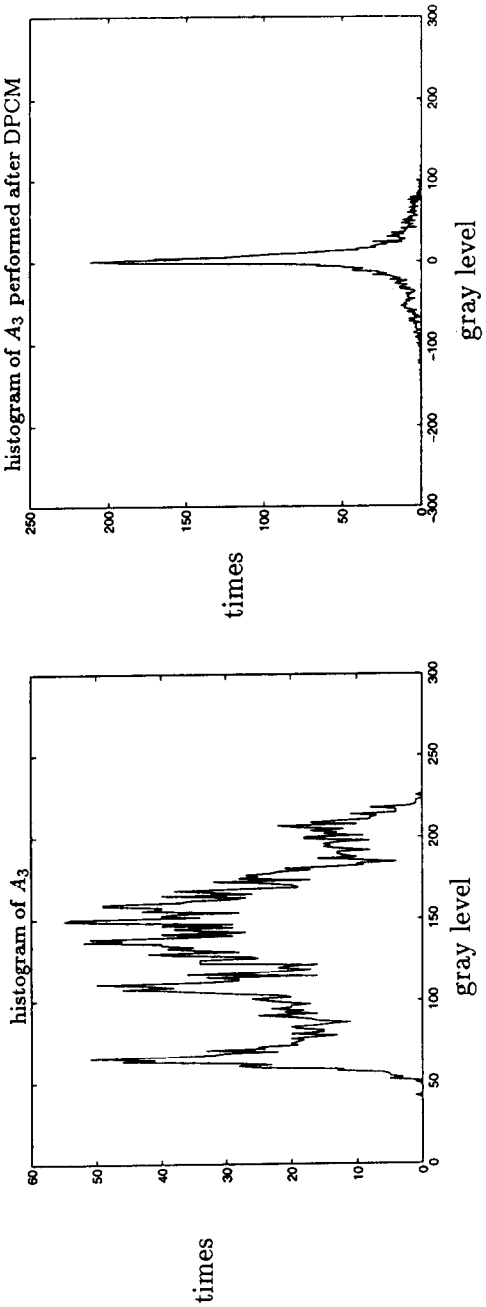

FIG. 9. Entropy and standard deviation reduction by DPCM: (a) histogram of A_3, (b) histogram of A_3^D.

TABLE II
Improvement of A_3 of Lena and Mandrill in CR, Entropy and Standard deviation by DPCM and HC

	$A_3+DPCM+HC$	A_3
Lena (δ = 10.6, RRLC)		
CR	37.8958	33.7439
Entropy	6.3334	7.2091
Standard deviation	27.5101	40.9785
Mandrill (δ = 19.7, RRLC)		
CR	17.6439	17.0753
Entropy	6.2357	7.0217
Standard deviation	20.0737	33.0999

respectively. Since the DWT has the properties of entropy reduction (7) and subband decomposition, the entropies and energy of the detailed images become small and the appearance of symbols are continuous. Hence, HC and RLC are useful to encode the output of the 3-level SQ performed after the DWT. For the case of Lena, the energy of detailed images is smaller than that of Mandrill. It implies that RLC has a better compaction in the case of Lena. Additionally, for each detailed image, the entropy depends on the sum of the original entropy and the logarithm of the relative energy (7). In the case of Mandrill, the entropies of the detailed images are larger than those of Lena since the original entropy and relative energy of Mandrill are both greater than those of Lena. It implies that HC can do better in the case of Lena than in the case of Mandrill. In addition, as δ increases, the increment of CR in RLC is better than that of HC since the contiguous area in spatial domain is expanded. See Fig. 10 for more details. Furthermore, the combination of RLC and HC, to obtain the benefit of these two methods, is introduced to increase CR. The difference of the CR between RLC+HC and RLC is by about 2 and 4 for the cases of Lena and Mandrill, respectively. RRLC achieves the best CR for both Lena and Mandrill, as illustrated in Fig. 10. The simulation results by HC, RLC, HC+RLC and RRLC are listed in Table 3 with the same PSNR.

4.4. *Increasing the decision levels of SQ*

After the 3-level scalar quantizer, the MSEs of these subimages are not the same, in general. The MSE of the lowest frequency component A_3 is due to the rounding effect. In the case of Lena, the differences of these errors, indicated in Table 4, are of the order of tens of thousands. We notice that, for the DWT, the MSEs are preserved by the fact that the energy conservation is sustained (7). That is, the sum of the mean squared errors in the DWT subimages is identical to that of the reconstructed image. Hence, we have the idea of increasing the number of decision levels for the subimages which yield larger MSE. In other words, we consider the cases of 4 levels or more scalar quantizers. In the detailed subimages of Lena, the energy decreases from the lower

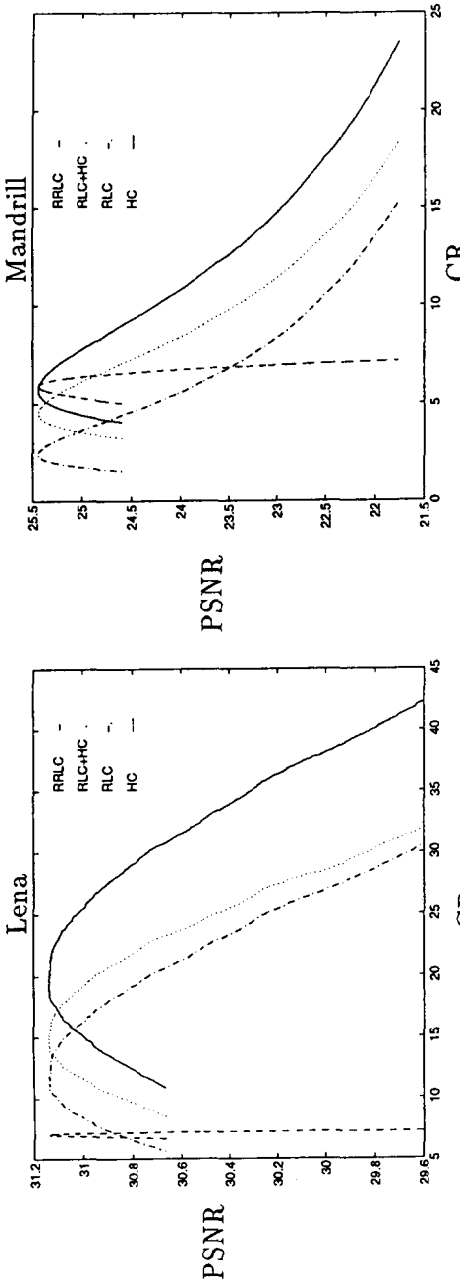

FIG. 10. PSNR vs CR by different coding methods (a) for Lena, δ increases from 3 to 12, (b) for Mandrill, δ increases from 3 to 24.

TABLE III
CR by using different coding methods in Lena and Mandrill

Coding method	HC	RLC	RLC+HC	RRLC
Lena ($\delta = 10.6$)	7.3061	26.7245	28.3713	37.8958
Mandrill ($\delta = 19.7$)	7.0608	10.5625	13.6207	17.6439

TABLE IV
Rounding error of A_3 and MSE of detailed images after a 3-level scalar quantizer

A_3	D_{h_3}	D_{v_3}	D_{d_3}	D_{h_2}	D_{v_2}	D_{d_2}	D_{h_1}	D_{v_1}	D_{d_1}
				Lena ($\delta = 10.6$)					
0.0831	15.1782	7.0310	6.4216	9.2220	4.8282	4.0593	5.6977	3.3646	1.8828
				Mandrill ($\delta = 19.7$)					
0.0841	37.5159	40.7976	27.7218	38.4230	51.7092	32.8934	32.8336	57.7964	24.4659

frequency to higher frequency components. Hence, we usually increase the numbers of decision levels in lower frequency components, e.g. D_3, to avoid losing PSNR too much. On the other hand, we reduce the rounding levels of A_3 since the rounding error is always smaller than other MSEs generated by the detailed images. After this improvement, the PSNR and CR are obviously lifted by about 1.5 and 2, respectively. In the case of Mandrill, the improvement is not clear since the energy of the higher frequency almost spreads out equally. That is, the energy of each component in detailed images is approximately equal. The PSNR vs CR curves are shown in Fig. 11.

4.5. *Comparisons with other methods*

The performance of several well-known compression techniques are compared with our method, as illustrated in Fig. 12. Our integrated compression method using the DWT is abbreviated as I_DWT. JPEG, which is the standard protocol of image compression, is broadly used in real applications. The discrete cosine transform (DCT) is adopted as the transformation technique. The quality of reconstructed images reduces rapidly when CR increases (**13**). When CR is over the value of 21, our method performs better than JPEG. The approach of vector quantization (VQ) is proposed by Gersho and Ramamurthi (**12**) to diminish the distortion induced by SQ and is indicated for comparison. Both PSNR and CR of VQ are not good. The revised method of VQ, entropy constrained vector quantization (ECVQ) (**11**), is also considered for comparison. The quality of decompressed picture is always lower than that of ours. Besides, the computation time and blocking effect are problems for implementation and the PSNR of ECVQ will descend in high compression ratios. Moreover, there are many recent publications on image compression using the idea of fractals, see (**14**) and page

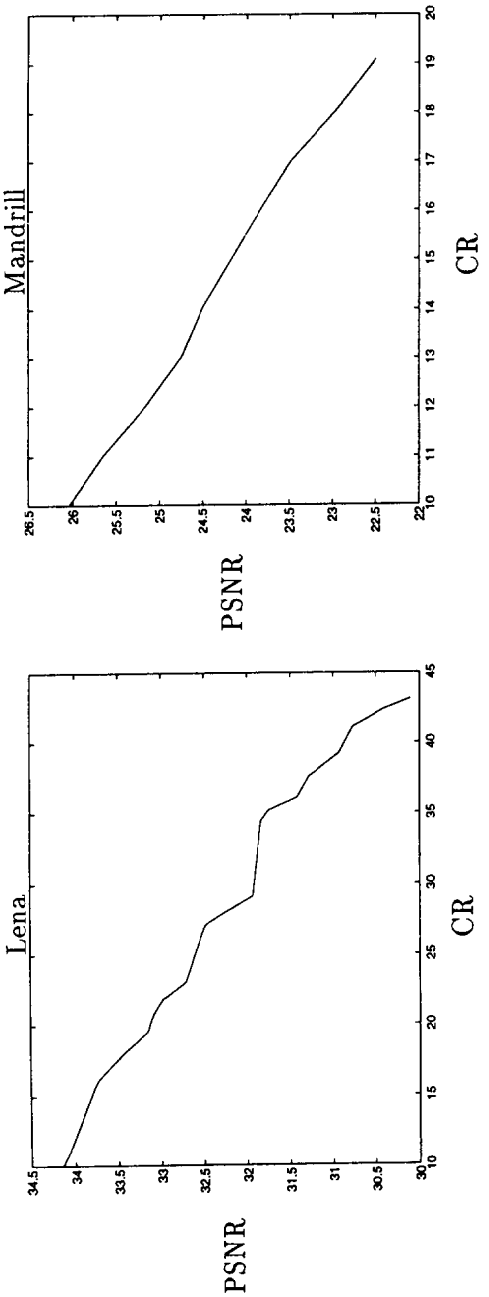

FIG. 11. The improvements of PSNR and CR after adding several decision levels and reducing the rounding levels of A_3.

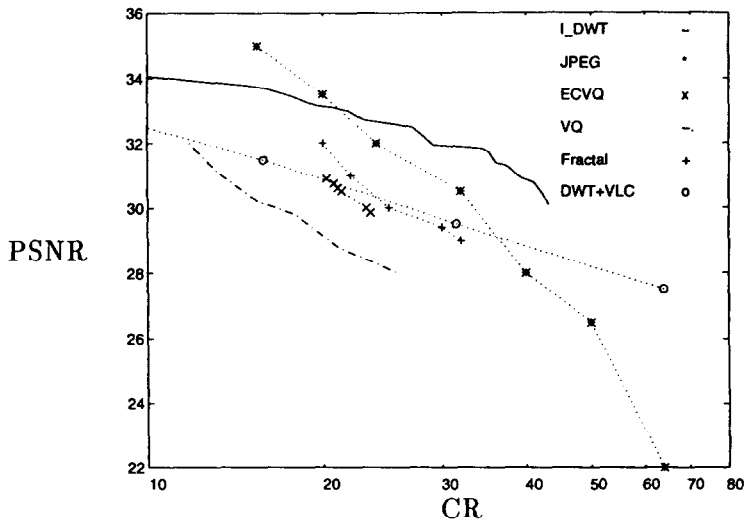

FIG. 12. Comparisons of the reconstructed image quality by several different approaches: integrated DWT (I_DWT), JPEG, ECVQ, VQ, Fractal, and DWT with variable-length coding (DWT + VLC).

73 of (**18**). This is performed by continuous contracted mapping to search for the best matching blocks from the domain and range pools. Preferable compression levels can be reached if the characteristics of the fractals in the original picture are rich enough. It needs much more time than the method of VQ to encode an image, and the blocking effect also appears if the choice of block size is not appropriate. The outcome of the fractal method is not superior to that of I_DWT, in general. Furthermore, there is an approach based on the DWT with variable-length coding (DWT + VLC) that can be regarded as a reference (**13**). This method also performs well in the case of low values of CR. Consequently, the PSNR vs CR curve of I_DWT is obviously higher than those of other methods when the values of CR are over 21.

V. Conclusion

We provide an integrated compression method which includes the discrete wavelet transform, scalar quantization and some lossless codings. The differential pulse code modulation is used to reduce the entropy of the lowest frequency subimage functioned after the discrete wavelet transform and to achieve high compression effects. The innovative approach, revised run-length coding, is proposed to save more bits for storage than the traditional run-length coding. In order to increase the image quality, we can increase the number of decision levels of scalar quantization or choose the vector quantization for further studies.

Acknowlegement

This work was supported by National Science Council under Grant NSC86-2213-E-009-066.

References

(1) Lim, J. S., *Two-Dimensional Signal and Image Processing*. Prentice-Hall, Englewood Cliffs, NJ, 1990.

(2) Baxes, G. A., *Digital Image Processing*. John Wiley and Sons, New York, 1994.

(3) Mallat, S. G., A theory for multiresolution signal decomposition: the wavelet representation. *IEEE Trans. Pattern Analysis and Machine Intelligence*, 1989, **11**, 674–693.

(4) Vetterli, M. and Kovačević, J., *Wavelets and Subband Coding*. Prentice-Hall, Englewood Cliffs, NJ, 1995.

(5) Akansu, A. N. and Smith, M. J. T., *Subband and Wavelet Transforms*. Kluwer Academic Publishers, Boston, Massachusetts, 1996.

(6) Woods, J. W. and O'Neil S. D., Subband coding of image. *IEEE Trans. Acoustics Speech and Signal Processing*, 1986, **34**, 1278–1288, October.

(7) Wu, B.-F. and Hsu, H.-H., Statistical properties and entropy reduction by discrete wavelet transforms. In *Proceedings of the* 1996 *International Symposium on Multi-Technology Information Processing*, Hsinchu, Taiwan, R.O.C., Dec. 1996, pp. 283–288.

(8) Strang, G. and Nguyen, T., *Wavelets and Filter Banks*. Wellesley-Cambridge, Cambridge, MA, 1996.

(9) Antonini, M., Barlaud, M., Mathieu, P. and Daubechies I., Image coding using wavelet transform. *IEEE Trans. Image Processing*, Vol. 1(2), April, pp. 205–220, 1992.

(10) Wu, B.-F. and Hsu, H.-H., Minimization of the scalar quantization error of discrete wavelet coefficients in image compression. Submitted to 1997 *IEEE International Symposium on Circuits and Systems*, Hong Kong.

(11) Chou, P. A., Lookabaugh, T. and Gray R. M., Entropy-constrained vector quantization. *IEEE Trans. Acoust. Speech and Signal Processing*, Vol. 37(1), pp. 31–42, 1989.

(12) Gersho, A. and Ramamurthi, B., Image coding using vector quantization. In *Proc. ICASSP*, Vol. 1, 1982, pp. 428–431.

(13) Hilton, M. L., Jawerth, B. D. and Sengupta A., Compressing still and moving images with wavelets. *Multimedia Systems*, 1994, **2**, 218–227.

(14) Jacobs, E. W., Fisher, Y. and Boss R. D., Image compression: a study of the iterated transform methods. *Signal Processing: Image Communication*, 1992, **29**, 251–263.

(15) Rabbani, M. and Jones, P. W., *Digital Image Compression Techniques*. SPIE Optical Engineering Press, Bellingham, Wash., 1991.

(16) Papoulis, A., *Probability, Random Variables, and Stochastic Processes*. 3rd edn. McGraw-Hill, Singapore, 1991.

(17) Wu, B.-F. and Hsu, H.-H., Entropy-constrained scalar quantization and minimum entropy with an error bound in wavelet-based image compression. Accepted by *IEEE Trans. Acoustics Speech and Signal Processing*.

(18) Fisher, Y., *Fractal Image Compression*. Springer, New York, 1995.

(19) Daubechies, I., Orthonormal bases of compactly supported wavelets. *Comm. Pure Appl. Math.*, 1988, **41**, 906–966.

(20) Daubechies, I., *Ten Lectures on Wavelets*. SIAM, Philadelphia, PA, 1992.

(21) Jung, K.-H. and Lee C. W., Image compression using projection vector quantization with quadtree decomposition. *Signal Processing: Image Communication*, 1996, **8**, 379–386.